

ENABLING ACCURATE LOW COST POSITIONING IN DENIED GPS ENVIRONMENTS WITH NONLINEAR ERROR MODELS OF INERTIAL SYSTEMS

Z. Shen ^a, J. Georgy ^a, M. Korenberg ^a, and A. Noureldin ^{b,*}

^a Department of Electrical and Computer Engineering, Queen's University, 19 Union Street, Walter Light Hall, Kingston, Ontario, K7L 3N6, Canada – (zhi.shen, j.georgy, korenber)@queensu.ca

^b Department of Electrical and Computer Engineering, Royal Military College of Canada / Queen's University, P.O.Box 17000 STN Forces, Kingston, Ontario, K7K 7B4, Canada – noureldin-a@rmc.ca

ISPRS WG I/5

KEY WORDS: INS/GPS Integration, Inertial Sensors, Fast Orthogonal Search, Kalman Filter, Vehicle Navigation

ABSTRACT:

The complementary characteristics of GPS and inertial sensors motivate their integration for more reliable positioning information in challenging GPS environments. Last decade has witnessed an increasing trend of utilizing MEMS-grade inertial sensors in the integration due to their low cost. For this research, only one MEMS-grade gyroscope and the vehicle built-in odometer are used together with two accelerometers to build a reduced inertial sensor system (RISS). This system is integrated with GPS to provide a low cost 3D positioning solution. As a linear estimation technique, Kalman Filter (KF) is adequate for the data fusion of GPS and high-end inertial sensors. However, MEMS-grade inertial sensors suffer from severe sensor errors including non-stationary stochastic drifts and nonlinear inertial errors, which undermine the effectiveness of KF. To overcome the problem, Fast Orthogonal Search (FOS) algorithm is employed in this research to identify the higher order RISS errors. With a tolerance of arbitrary stochastic noise, FOS is able to build an accurate nonlinear model that predicts RISS errors. KF can then be augmented by FOS to estimate and reduce both linear and nonlinear inertial errors, thus enhancing the navigation performance. The road test trajectory is conducted to examine the proposed method. The results demonstrate the advantages of the proposed method over the stand alone KF approach.

1. INTRODUCTION

Nowadays, Global Positioning System (GPS) is commonly utilized to achieve land vehicle navigation. However, in urban canyons, tunnels, and the other GPS-denied environments, possible signal blockage may jeopardize the availability of GPS information (Farrell, 1998). To establish a more reliable positioning system, GPS needs to work together with a standalone inertial navigation system (INS). Linear estimation techniques such as Kalman filter (KF) are always used to conduct the INS/GPS integration (Hostetler and Andreas, 1983; Grewal et al., 2007). When GPS signals are available, KF predicts INS errors according to the previous estimation and corrects them using GPS updates. Once GPS outages occur, KF operates in the prediction mode. It predicts and removes the linear INS errors relying on the linearized dynamic model of INS error states as well as the first order stochastic model of the inertial sensor errors (Noureldin et al., 2004). As a result, the unaided INS data can be corrected. The system is thus able to maintain the availability and the accuracy of positioning.

Owing to the rapid booming Micro-Electro-Mechanical System (MEMS) technologies, the MEMS-based inertial measurement unit (IMU) becomes popular because of its low cost. Other advantages like low power consumption and small size (Barbour and Schmidt, 2001) make MEMS IMU preferred by recent cost-sensitive vehicle navigation systems. Currently, MEMS-based INS is challenged by intensive nonlinear INS errors and non-stationary MEMS sensor errors. Although, by removing linear system errors, KF is adequate to keep the positioning accuracy of the higher grade INS, it has limited

success when applied to the MEMS-based system. In such cases, there are massive nonlinear INS errors, which cannot be handled by KF. Once the GPS aiding is unavailable, these errors may grow over time without boundary. Eventually, their effects can undermine the overall positioning accuracy seriously. How to prevent the above scenario motivates the nonlinear modelling of INS errors.

This paper aims at improving MEMS-based INS/GPS integration by handling nonlinear INS errors. Fast Orthogonal Search (FOS) algorithm is adopted to establish the higher order error model. It updates the model structure continuously using GPS readings while available. Should GPS outages occur, the pre-built FOS model is applied to predict the higher order INS errors. The system performance can then be improved in terms of the above predictions. To examine the proposed method, a MEMS-based reduced inertial sensor system (RISS) is employed for the testing. Instead of using a Six Degree of Freedom (6DoF) Full IMU, RISS offers 2D/3D navigation solution using fewer MEMS sensors. 2D RISS was firstly proposed by Iqbal et al., 2008. It relies on a MEMS grade gyroscope aligned along the vertical direction and the vehicle built-in odometer integrated with GPS using KF to provide a low cost 2D positioning solution on the horizontal plane. Iqbal et al., 2008 also proposed adding two accelerometers to calculate the pitch and roll which were independent of the positioning solution. Georgy et al., 2010 augmented 2D RISS by adding a more accurate calculation of the pitch and roll inside the integration filter to obtain a full 3D navigation solution. Since the pitch and roll calculations were used in turn

* Corresponding author

to determine the vertical velocity and position, a 3D positioning solution can be obtained in this manner. 3D RISS/GPS integration was explored and achieved using either Particle Filter (Georgy et al., 2010) or tightly coupled KF (Tashfeen et al., 2009). In this paper, KF is still utilized to execute RISS/GPS integration in a loosely coupled scheme. The proposed method (FOS) is cascaded to KF in order to suppress nonlinear INS errors.

Section 2 discusses 3D RISS and its error model. In Section 3, the FOS algorithm is reviewed and introduced to the modelling of nonlinear RISS errors. The experimental results are presented in Section 4.

2. RISS ERRORS IN 3D VEHICLE NAVIGATION

2.1 Three Dimensional RISS Mechanization

The ultimate goal of RISS is to keep a balance between the system cost and navigation functionality. A low cost 2D RISS proposed by Iqbal et al., 2008, consists of a single axis gyroscope and a vehicle built-in odometer. The gyroscope is installed with its sensitive axis along the vertical direction of the vehicle. With the assumption that the vehicle mostly travels on the horizontal plane, its velocities along the North and the East can be determined using the vehicle forward speed and the heading angle obtained by the odometer and the gyroscope, respectively. The velocities can then be integrated over time to derive the latitude and longitude of the vehicle. This former work also proposed the use of two accelerometers, which point towards the forward and transverse directions, to compute the pitch and roll independently of the positioning solution. To offer a full 3D positioning solution, Georgy et al., 2010 suggested to augment the above system by exploiting the pitch and roll calculation using the two accelerometers to get more accurate horizontal position and velocity as well as vertical velocity and altitude. The measurements of these accelerometers are used together with the odometer-derived speed and a reliable gravity model to determine the pitch and roll of the vehicle. Consequently, one can calculate the vertical velocity of the vehicle using the pitch and the forward speed. The altitude of the vehicle can then be derived as well. The 3D RISS used in this paper includes a MEMS grade single axis gyroscope, a vehicular odometer, and two MEMS grade single axis accelerometers. It is integrated with a GPS receiver and works in the above-mentioned manner. The following figure demonstrates how it derives 3D positioning results in terms of the inertial measurements. This procedure is also known as 3D RISS mechanization.

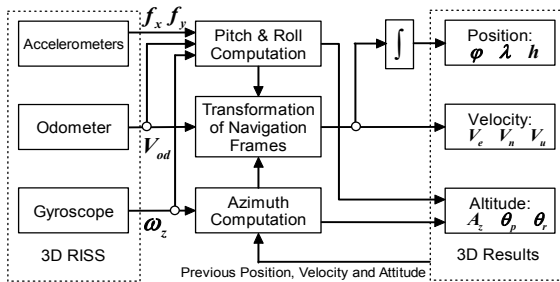


Figure 1. Block diagram of 3D RISS mechanization

In Figure 1, by removing effects of the Earth rotation ω_e and the change of orientation of the local level frame with respect to the Earth, the azimuth A_z can be determined as Eq (1):

$$\dot{A}_z = -(\omega_z - \omega_e \sin \varphi - \frac{V_e \tan \varphi}{R_N + h}) \quad (1)$$

where ω_z = vertical aligned gyroscope measurement;

φ = latitude; h = altitude;

V_e = velocity along the East;

R_N = normal radius of curvature of the Earth's ellipsoid.

Using the azimuth A_z , the pitch θ_p , and the forward speed V_{od} (measured by the odometer), the vehicular velocities along the East and the North (V_e and V_n) can then be derived in Eq (2).

$$\begin{pmatrix} V_e \\ V_n \end{pmatrix} = \begin{pmatrix} V_{od} \sin A_z \cos \theta_p \\ V_{od} \cos A_z \cos \theta_p \end{pmatrix} \quad (2)$$

The latitude φ and longitude λ of the vehicle can be determined in Eq (3) as well:

$$\begin{pmatrix} \varphi \\ \lambda \end{pmatrix} = \begin{pmatrix} 0 & \frac{1}{R_M + h} \\ \frac{1}{(R_N + h) \cos \varphi} & 0 \end{pmatrix} \begin{pmatrix} V_e \\ V_n \end{pmatrix} \quad (3)$$

where R_M = meridian radius of curvature of the Earth's ellipsoid.

The pitch and roll are computed in terms of the idea presented by Noureldin et al., 2002 and Georgy et al., 2010. When the vehicle is stationary, the accelerometers measure components of the gravity due to the pitch and roll angles (tilt from the horizontal plane). When the vehicle is moving, the forward accelerometer measures both the forward vehicle acceleration and the component of the gravity. To determine the pitch angle, the vehicle acceleration derived from odometer measurements should be deducted from the forward accelerometer measurement. Also, the transversal accelerometer measures the normal part of the vehicle acceleration as well as the component of the gravity. Hence, to derive the roll angle, the transversal accelerometer measurement should be compensated for the normal part of the vehicular acceleration. As a result, the pitch θ_p and the roll θ_r can be determined by Eq (4):

$$\theta_p = \arcsin\left(\frac{f_y - a_{od}}{g}\right), \quad \theta_r = -\arcsin\left(\frac{f_x + V_{od}\omega_z}{g \cos \theta_p}\right) \quad (4)$$

where g = gravity acceleration;

f_x = transversal accelerometer measurement;

f_y = forward accelerometer measurement;

a_{od} = vehicle acceleration derived from V_{od} .

The vertical velocity (V_u) and the altitude (h) of the vehicle can then be derived using Eq (5).

$$\begin{pmatrix} V_u \\ \dot{h} \end{pmatrix} = \begin{pmatrix} V_{od} \sin \theta_p \\ V_u \end{pmatrix} \quad (5)$$

2.2 RISS Error Model

The RISS error state vector δX consists of position errors ($\delta \phi$, $\delta \lambda$, δh), velocity errors (δV_e , δV_n , δV_u), azimuth errors δA_z , and sensor measurement errors (δa_{od} , $\delta \omega_z$). Since these errors are variable in time, they can be described by differential equations. By applying Taylor series approximation on Eq (1) – (5) or their time derivative, one can establish the error model of 3D RISS to be used inside the KF. For instance, one can derive the error models of the azimuth, velocities, and position as Eq (6) – (8):

$$\delta \dot{A}_z = \delta \omega_z + \Delta A_z \quad (6)$$

$$\begin{pmatrix} \delta \dot{V}_e \\ \delta \dot{V}_n \\ \delta \dot{V}_u \end{pmatrix} = \begin{pmatrix} \sin A_z \cos \theta_p & a_{od} \cos A_z \cos \theta_p & 0 \\ \cos A_z \cos \theta_p & -a_{od} \sin A_z \cos \theta_p & 0 \\ \sin \theta_p & 0 & a_{od} \cos \theta_p \end{pmatrix} \begin{pmatrix} \delta a_{od} \\ \delta A_z \\ \delta \theta_p \end{pmatrix} + o \begin{pmatrix} \delta a_{od} \\ \delta A_z \\ \delta \theta_p \end{pmatrix} \quad (7)$$

$$\begin{pmatrix} \delta \dot{\phi} \\ \delta \dot{\lambda} \\ \delta \dot{h} \end{pmatrix} = \begin{pmatrix} 0 & \frac{1}{R_M + h} & 0 \\ \frac{1}{(R_N + h) \cos \phi} & 0 & 0 \\ 0 & 0 & 1 \end{pmatrix} \begin{pmatrix} \delta V_e \\ \delta V_n \\ \delta V_u \end{pmatrix} + o \begin{pmatrix} \delta V_e \\ \delta V_n \\ \delta V_u \end{pmatrix} \quad (8)$$

where ΔA_z and $o(\cdot)$ denote corresponding higher order residual errors. The sensor errors are described as 1st order Gauss-Markov models.

According to Eq (1) – (5), in 3D RISS, only the azimuth, the pitch and the roll depend on the measurements of MEMS grade inertial sensors directly. Since the pitch and roll calculations from the accelerometers do not include integration operations, these angles do not suffer from error growth with time due to the integration. On the other hand, the azimuth suffers heavily from the stochastic sensor errors of the MEMS grade gyroscope and the nonlinear inertial system errors (Noureldin et al., 2009). Although the linear part of azimuth errors can be removed by KF, its higher order residual errors (ΔA_z) still exist and may accumulate over time. They can deteriorate the overall RISS accuracy seriously and, therefore, require the nonlinear analysis.

In case of the vehicular navigation, due to the possible misalignment and system error propagation, ΔA_z may depend on the power or cross products of the linear error state elements (δX) as well. Thus, the discrete version of Eq (6) can be described as Eq (9), where $P_m(n)$ contains arbitrary powers or

cross products of current or previous error state elements (including the linear part of rotation rate error $\delta \omega_z$); $e(n)$ represents the residual.

$$\begin{aligned} \frac{\delta A_z(n) - \delta A_z(n-1)}{\Delta t} &= \delta \omega_z(n) + \Delta A_z \\ &= \sum_{m=0}^M \alpha_m P_m(n) + e(n) \end{aligned} \quad (9)$$

Once all the $P_m(n)$ and their weight coefficients α_m are figured out, the nonlinearity of the azimuth error model can be uniquely identified.

3. FOS-BASED NONLINEAR MODELLING OF RISS ERRORS

3.1 Fast Orthogonal Search Algorithm

Fast Orthogonal Search (FOS) was introduced by Korenberg, 1987. It is a general-purpose algorithm to build the difference equation or functional expansion representations of systems with unknown structure (Korenberg, 1987). Without loss of generality, any nonlinear systems can be approximated as Eq (10), where $P_m(n)$ are possible candidate terms; $x(n)$ and $y(n)$ are system inputs and outputs, respectively; N_0 denotes the maximum system delay.

$$\begin{aligned} y(n) &= \sum_{m=0}^M a_m P_m(n) + e(n); \\ P_m(n) &= y(n-k_0) \cdots y(n-k_i) x(n-l_0) \cdots x(n-l_j), \quad (10) \\ m \geq 1, i \geq 0, j \geq 0; P_0(n) &= 1; \\ \forall i : 1 \leq k \leq N_0; \forall j : 0 \leq l_j \leq N_0 \end{aligned}$$

FOS essentially establishes a nonlinear model of $y(n)$ using an arbitrary set of $P_m(n)$. To achieve this, it performs the orthogonal searching on a functional expansion to produce an economical orthogonal series (Korenberg, 1989):

$$y(n) = \sum_{m=0}^M g_m w_m(n) + e(n) \quad (11)$$

where g_m are the weights of the orthogonal functions in sense of least-mean-square model-fit; $e(n)$ is the residual error; orthogonal functions $w_m(n)$ can be derived from the non-orthogonal candidates $P_m(n)$ using the Gram-Schmidt orthogonalization. The advantage of FOS here is that it is able to compute g_m without explicitly deriving $w_m(n)$, thus saving lots of system memory space and the calculation time. By implicitly decomposing the nonlinear system output $y(n)$ in an orthogonal function space defined by $\{w_m(n)\}$, FOS systematically examines each possible candidate term $P_m(n)$. It selects the best one to include in the model such that this candidate offers the maximum reduction of model-fit mean-

square-errors (*m.s.e.*) defined in Eq (12). The over-bar denotes the time average from $n = N_0$ to $n = N$.

$$m.s.e. = \overline{e^2(n)} = \overline{y^2(n)} - \sum_{m=0}^M \overline{g_m^2 w_m^2(n)} \quad (12)$$

Recursively, the updated *m.s.e.* is fed back to conduct the next iteration of searching till the stopping criteria have been met. Eventually, an accurate system model is reconstructed from the orthogonal function space. More details about FOS can be found in the references (Korenberg, 1987; Korenberg, 1989; Paarmann and Korenberg, 1992).

3.2 Application of FOS to 3D RISS/GPS Integration

To reduce both linear and nonlinear RISS errors, an augmented KF/FOS module is suggested. During GPS availability, the KF operates in a standard loosely coupled style to conduct 3D RISS/GPS data fusion. In parallel, its prediction of linear azimuth error δA_z^{KF} can be used together with mechanization results A_z^{mec} and GPS aiding A_z^{gps} to compute the true nonlinear azimuth error $\Delta A_z = A_z^{mec} - \delta A_z^{KF} - A_z^{gps}$. As the desired model output, ΔA_z is used to train the FOS modelling of higher order azimuth errors. Also, all the KF predictions are sent to FOS to construct the possible candidates. Figure 2 depicts the procedure of FOS training stage.

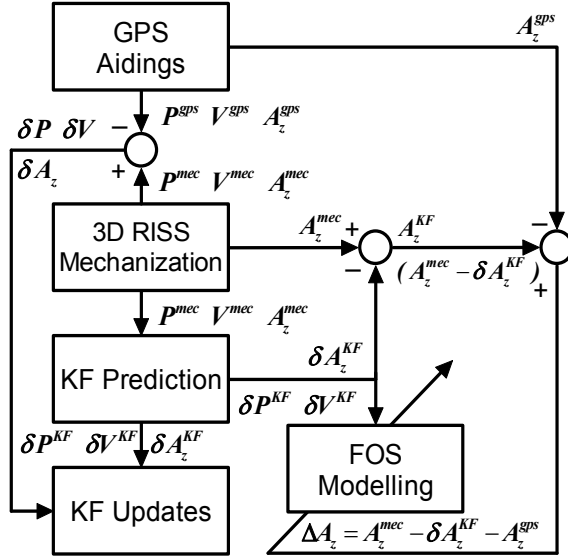


Figure 2. FOS training stage

During GPS outages, the FOS module works in prediction scheme. The pre-built FOS model predicts nonlinear azimuth error ΔA_z^* from KF estimations. ΔA_z^* can then be used together with KF prediction δA_z^{KF} and the original mechanization result A_z^{mec} to derive corrected azimuth A_z^* in Eq (13).

$$A_z^* = A_z^{mec} - \delta A_z^{KF} - \Delta A_z^* \quad (13)$$

Finally, another standalone 3D RISS mechanization can start and benefit from the feeding of A_z^* . It is supposed to offer more accurate position P^* and velocities V^* .

4. EXPERIMENTAL RESULTS

The proposed method was examined with road test experiments in a land vehicle. The gyroscope and two accelerometers used in this research are from a Crossbow MEMS grade IMU300CC-100. The on-board diagnostic version II (ODB II) interface was utilized to log in the odometer readings. The results of the proposed navigation solution are evaluated with respect to a reference solution offered by NovAtel G2 Pro-Pack SPAN unit. In this high-end module, a Honeywell HG1700 tactical grade IMU is integrated with the GPS receiver in a tightly coupled scheme developed by NovAtel. See Table 1 and Table 2 to compare the performances of low cost Crossbow MEMS grade IMU and Honeywell's high-end tactical grade IMU.

Crossbow IMU300CC (MEMS grade IMU)			
Z-Axis Gyroscope		X/Y-Axis Accelerometers	
Bias (deg/sec)	< +/- 2.00	Bias (mg)	< +/- 30.00
Scale Factor (%)	< 1.000	Scale Factor (%)	< 1.000
Random Walk (deg/hr ^{1/2})	2.250	Random Walk (m/(s-hr ^{1/2}))	0.150

Table 1. Bias, scale factor and random walk of Crossbow IMU

Honeywell HG1700 (Tactical grade IMU)			
Gyroscopes		Accelerometers	
Bias (deg/hr)	< 1.000	Bias (mg)	< 1.000
Scale Factor (ppm)	< 150.000	Scale Factor (ppm)	< 300.000
Random Walk (deg/hr ^{1/2})	< 0.125	Random Walk (m/(s-hr ^{1/2}))	N/A

Table 2. Bias, scale factor and random walk of HG1700 IMU

The trajectory used in this paper, shown in Figure 3, was carried out in the suburbs of Kingston, Ontario, Canada. It includes several urban streets and suburb roads around Kingston as well as parts of the nearby highway. The road test lasted for about 80 minutes of continuous vehicle travel and a distance over 75 kilometres. To examine the KF/FOS performance in denied GPS environments, up to seven artificial GPS outages of 120 seconds each (indicated by circle overlaid on the map in Figure 3) were intentionally introduced such that they involve straight portions and turns. A 60-second sliding window is used for the FOS modelling.

Figure 4 and Table 3 show the maximum errors in the estimated horizontal position during the seven 120-second GPS outages for both KF-only and KF/FOS methods. Clearly, during all the GPS outages, KF/FOS performs better than KF-only in the reduction of horizontal position errors. In case of sharp turns (GPS outage #1, #2, #4), lower speeds with stops (GPS outage #7), and higher speeds (GPS outage #3), the proposed approach provided more than 50% accuracy enhancement over the KF-only solution. Most of the improvement relies on the FOS-based reduction of relatively larger nonlinear azimuth errors. In fact, as shown in Eq (6) – (8), the azimuth error mainly

influences the accuracy of horizontal velocities and position instead of vertical navigation parameters. This explains why the KF/FOS method used in this paper is more successful in horizontal positioning.



Figure 3. Kingston suburb trajectory

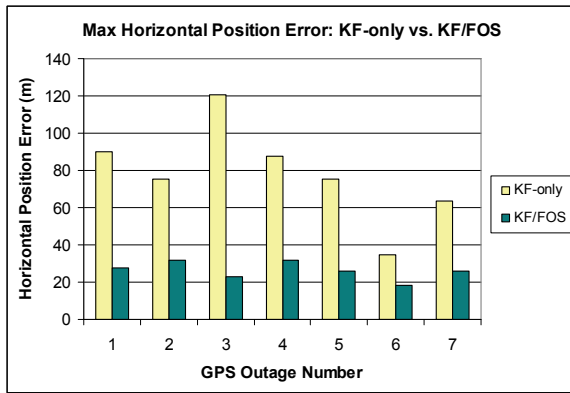


Figure 4. Maximum horizontal position error of KF-only and KF/FOS methods during 120-second GPS outages

GPS outage #	KF-only Max Pos. Err. (m)	KF/FOS Max Pos. Err. (m)	KF/FOS improve (%)
1	90.16	27.62	69.37
2	75.21	31.81	57.71
3	120.32	22.97	80.91
4	87.61	31.83	63.67
5	75.09	25.78	65.67
6	34.99	18.38	47.47
7	63.31	25.80	59.25
Average	78.10	26.31	66.31

Table 3. Maximum horizontal position error of KF-only and KF/FOS methods during 120-second GPS outages

In GPS outage #1 (shown in Figure 5), while decelerating from a speed around 75 km/hr to a stop (shown in Figure 6), the vehicle experienced an 110° turn at an average speed of 65.70 km/hr. The maximum position errors of KF/FOS and KF-only methods are 27.62 meters and 90.16 meters, respectively. The over 69% accuracy enhancement in horizontal position demonstrates the advantage of FOS-based reduction of nonlinear azimuth errors. This advantage was confirmed again in GPS outage #2 and #4, where the vehicle conducted a 125° turn and a 95° turn, respectively. In both cases, the KF/FOS

solution shows superior performance by introducing over 55% accuracy enhancement in horizontal position over KF-only solution. All the above results verified the effectiveness of KF/FOS in case of sharp turns.

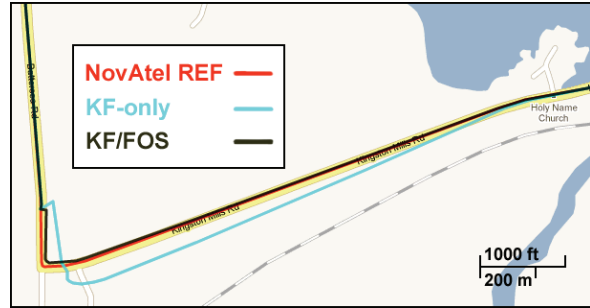


Figure 5. Performance during GPS outage #1

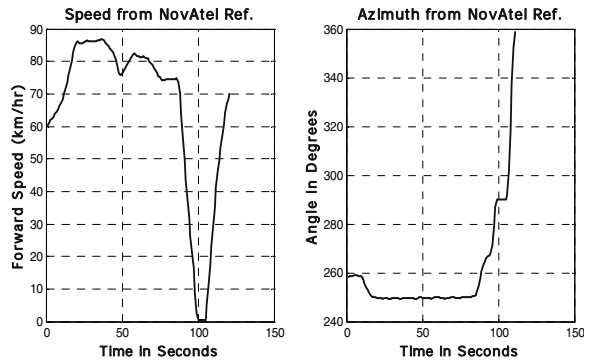


Figure 6. Speed and Azimuth during GPS outage #1

To evaluate the KF/FOS performance in case of higher speeds, GPS outage #3 (shown in Figure 7) is examined. During this outage, the vehicle firstly accelerated from a speed over 80 km/hr to reach the highway and then kept on a high speed over 105 km/hr (See Figure 8). It conducted a 70° turn when entering the highway as well. The maximum horizontal position error of KF-only here is 120.32 meters. KF/FOS method decreases this value to 22.97 meters and offers more than 80% accuracy enhancement. This demonstrates the great advantages of KF/FOS at providing reliable navigation performance even in case of high vehicle speeds with headings angle dynamics.

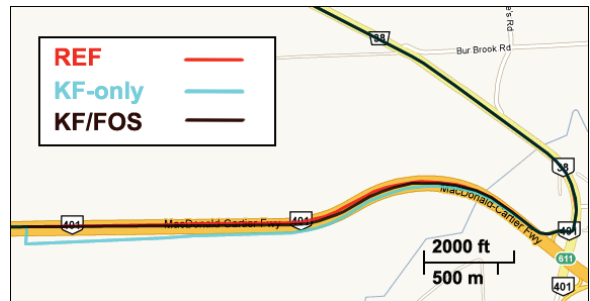


Figure 7. Performance during GPS outage #3

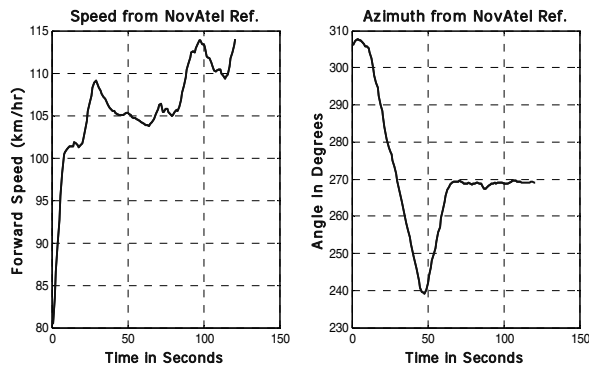


Figure 8. Speed and Azimuth during GPS outage #3

5. CONCLUSION

This paper explored an enhanced approach to a low cost 3D vehicular navigation system using a MEMS grade gyroscope, a vehicle built-in odometer, two single axis MEMS grade accelerometers, and a GPS receiver. Owing to its ability of detecting and reducing nonlinear inertial errors, FOS was proposed to be cascaded to KF and was used to conduct MEMS grade RISS/GPS integration. The road test experimental results show that the proposed method is able to correct the nonlinear RISS errors such as higher order azimuth errors and horizontal position errors. This enables the KF/FOS solution to provide superior navigation accuracy over KF-only approach during GPS outages with different vehicle dynamics.

ACKNOWLEDGEMENT

This research was supported in part by research grants from Natural Sciences and Engineering Research Council (NSERC), Geomatics for Informed Decision (GEOIDE) Network Centers of Excellence, and Defence Research and Development Canada (DRDC) Ottawa. The equipment was acquired by research funds from Canada Foundation for Innovation, Ontario Innovation Trust and the Royal Military College of Canada.

REFERENCES

- Barbour, N. and Schmidt, G., 2001. Inertial Sensor Technology Trends, *IEEE Sens. J.*, 1(4), pp. 332 – 339.
- Farrell, J.A. and Barth, M., 1998. *The Global Positioning System and Inertial Navigation*, McGraw Hill, USA.
- Georgy, J., Noureldin, A., Korenberg, M., and Bayoumi, M., 2010. Low Cost 3D Navigation Solution for RISS/GPS Integration Using Mixture Particle Filter, *IEEE Transaction on Vehicular Technology*, 59(2), pp. 599-615.
- Grewal, M.S., Weill, L. R., and Andrews, A.P., 2001. *Global Positioning Systems, Inertial Navigation, and Integration*, John Wiley and Sons, USA.
- Hostetler, L. and Andreas, R., 1983. Nonlinear Kalman Filtering Techniques for Terrain-aided Navigation, *IEEE Transaction on Automatic Control*, 28(3), PP. 315 – 323.
- Iqbal, U., Okou, A.F., and Noureldin, A., 2008. An Integrated Reduced Inertial Sensor System – RISS/GPS for Land Vehicle, Position, Location and Navigation Symposium (PLANS), Monterey, CA, USA, pp. 1014 – 1021.
- Karamat, T.B., Georgy, J., Iqbal, U., and Noureldin, A., 2009. A Tightly-Coupled Reduced Multi-Sensor System for Urban Navigation, 22nd International Meeting of the Satellite Division of The Institute of Navigation (ION GNSS 2009), Savannah, GA, USA, pp. 582 – 592.
- Korenberg, M.J., 1987. Fast Orthogonal Identification of Nonlinear Difference Equation Models, *Proc. 30th Midwest Symposium on Circuits and Systems*, Syracuse, NY, USA, 1, pp. 270 – 276.
- Korenberg, M.J., 1989. A Robust Orthogonal Algorithm for System Identification and Time Series Analysis, *Biol. Cybern.*, 60, pp. 267 – 276.
- Noureldin, A., Irvine-Halliday, D., and Mintcheve, M.P., 2002. Accuracy Limitations of FOG-Based Continuous Measurement-While-Drilling Surveying Instruments for Horizontal Wells, *IEEE Transaction on Instrumentation and Measurements*, 51(6), pp. 1177 – 1190.
- Noureldin, A., Karamat, T.B., Eberts, M.D., and El-Shafie, A., 2009. Performance Enhancement of MEMS-Based INS/GPS Integration for Low-Cost Navigation Applications, *IEEE Transaction on Vehicular Technology*, 58(3), pp. 1077 – 1096.
- Noureldin, A., Nassar, S., and El-Sheimy, N., 2004. A Neuro-Wavelet Method for Multi-sensor System Integration for Vehicular Navigation, *J. Meas. Sci. Technol.*, 15(2), pp. 404 – 412.
- Paarmann, L.D. and Korenberg, M.J., 1992. Estimation of the Parameters of an ARMA Signal Model Based on an Orthogonal Search, *IEEE Transaction on Automatic Control* 37(3), pp. 347 – 352.